

1           **A toolkit for converting Gal4 into LexA and Flippase transgenes in *Drosophila***

2   Sasidhar Karuparti<sup>1,2,3</sup>, Ann T. Yeung<sup>1,3</sup>, Bei Wang<sup>1</sup>, Pedro F. Guicardi<sup>1</sup>, Chun Han<sup>1,\*</sup>

3   <sup>1</sup>Weill Institute for Cell and Molecular Biology and Department of Molecular Biology and

4   Genetics, Cornell University, Ithaca, NY 14853, USA

5   <sup>2</sup>Current address: School of Medicine, University of Missouri, Columbia, MO 65212, USA

6   <sup>3</sup>These authors contributed equally to this work

7   \*Correspondence and Lead Contact: [chun.han@cornell.edu](mailto:chun.han@cornell.edu)

8   **Running Title**

9   Conversion of Gal4 to LexA and Flippase

10   **Keyword**

11   Gal4, LexA, Flippase, HACK, CRISPR, *Drosophila*, tools

## 12 Abstract

13 *Drosophila* has been a powerful model system for biological studies due to the wide range of  
14 genetic tools established for it. Among these tools, Gal4 is the most abundant, offering  
15 unparalleled tissue- and developmental stage-specificity for gene manipulation. In comparison,  
16 other genetic reagents are far fewer in choices. Here we present a genetic toolkit for converting  
17 Gal4 strains into LexA and Flippase transgenes through simple genetic crosses and fluorescence  
18 screening. We demonstrate the proof-of-principle by converting ten Gal4 lines that exhibit  
19 diverse tissue specificities and examined the activity patterns of the converted LexA and  
20 Flippase lines. Gal4-to-LexA and Flp conversion is fast and convenient and should greatly  
21 expand the choices of LexA and Flp for binary expression and FRT-based mosaic analysis,  
22 respectively, in *Drosophila*.

23

## 24 Introduction

25 *Drosophila* is a powerful model system for studying developmental biology, cell biology,  
26 neurobiology, and genetics. This power largely lies in the numerous genetic tools available in  
27 *Drosophila* for manipulating the genome and gene activity. Commonly used tools include binary  
28 gene expression systems (BRAND AND PERRIMON 1993; LAI AND LEE 2006; POTTER *et al.* 2010),  
29 site-specific recombinases (GOLIC AND LINDQUIST 1989; BISCHOF *et al.* 2007; NERN *et al.* 2011),  
30 clustered regularly-interspaced palindromic repeats (CRISPR)/Cas9 (GRATZ *et al.* 2013; EWEN-  
31 CAMPEN *et al.* 2017; BOSCH *et al.* 2020; BOSCH *et al.* 2021), and many more. Binary expression  
32 systems allow for expression of transgenes in spatially and temporally restricted, and  
33 developmental stage-specific manners. Their variants (OSTERWALDER *et al.* 2001; LUAN *et al.*  
34 2006) and modifiers (MCGUIRE *et al.* 2003) further increase the precision of the control and offer  
35 greater flexibility. Site-specific recombination systems enable rearrangement of genomic DNA  
36 and allow for development of sophisticated methods for creating genetic mosaics (DANG AND  
37 PERRIMON 1992; STRUHL AND BASLER 1993; XU AND RUBIN 1993; LEE AND LUO 1999). More  
38 recently, CRISPR/Cas9 tools allow convenient generation of permanent or tissue-specific  
39 mutations (GRATZ *et al.* 2013; PORT *et al.* 2014; POE *et al.* 2017), replacement of endogenous  
40 genomic sequences with desired ones (GRATZ *et al.* 2014; PORT *et al.* 2014), and insertion of  
41 exogenous sequences at precise loci (LEE *et al.* 2018).

42 Since the introduction of the yeast Gal4/UAS system into *Drosophila* (BRAND AND  
43 PERRIMON 1993), tens of thousands of Gal4 strains have been generated using diverse  
44 approaches (BRAND AND PERRIMON 1993; SHARMA *et al.* 2002; PFEIFFER *et al.* 2008; JENETT *et*  
45 *al.* 2012; KVON *et al.* 2014). In each strain, the transcription factor Gal4 is expressed under the  
46 control of specific enhancer elements and thus exhibits a unique expression pattern. This vast  
47 Gal4 resource makes investigations of gene function feasible in virtually any tissue and at any  
48 developmental stage. In comparison, the availability of other genetic tools is much more limited,  
49 hampering researchers' ability to use orthogonal approaches. For example, LexA/LexAop is  
50 another popular binary system (LAI AND LEE 2006), but the limited choices for LexA make the

51 system less flexible to use as compared to Gal4. Flp/FRT is a site-specific recombination system;  
52 it enables mosaic analysis techniques such as flp-out (STRUHL AND BASLER 1993) and MARCM  
53 (LEE AND LUO 1999). Although temporally inducible Flp is available for these techniques, tissue-  
54 specific Flp would greatly simplify and streamline large-scale applications such as genetic  
55 screens (HUANG *et al.* 2014; NEUKOMM *et al.* 2014). However, tissue-specific Flp resources are  
56 also very limited at present. Thus, convenient methods for generating additional tissue-specific  
57 LexA and Flp lines will be greatly beneficial to the *Drosophila* research community.

58 CRISPR/Cas9 provides an attractive option for converting existing Gal4 resources into  
59 other systems. It has been widely used in *Drosophila* for precise genome engineering (GRATZ *et*  
60 *al.* 2014; PORT *et al.* 2014), which takes advantage of double-strand break (DSB)-induced DNA  
61 repair through the homologous recombination pathway. While it is common to perform gene  
62 replacement through embryo injections, the recently developed homology assisted CRISPR  
63 knock-in (HACK) method demonstrated the feasibility of converting existing Gal4 lines into  
64 other tissue-specific reagents through simple genetic crosses (LIN AND POTTER 2016). This  
65 method eliminates the need for injection because the necessary genetic components are brought  
66 together by genetic crosses to induce homologous recombination in the fly germline. This  
67 method has already been successfully used to convert Gal4 strains into tissue-specific QF, split-  
68 Gal4, Gal80, and Cas9 lines (LIN AND POTTER 2016; XIE *et al.* 2018; CHEN *et al.* 2020;  
69 KOREMAN *et al.* 2021). Although HACK has the potential to greatly expand available genetic  
70 resources for researchers, this method has not been used to make LexA or Flp reagents, which  
71 would be useful complementary tools to the ones previously made.

72 In this study, we developed tools that allow conversion of Gal4 lines into LexA and Flp  
73 lines based on HACK. We demonstrate the proof-of-principle by converting several Gal4 drivers  
74 that are expressed in stem cells, epithelial cells, muscles, adipocytes, glia, and neurons. We show  
75 that the tissue-specificity of these LexA and Flp reagents is maintained. This method is  
76 convenient and can be applied at a large scale for rapid expansion of LexA and Flp resources.

## 77 Materials and Methods

### 78 Fly strains

79 The fly strains used in this study are listed in the Reagent Table.

### 80 Construction of HACK donor vectors

81 The HACK donor vectors were constructed by modifying pHACK(Gal4)-DONR(T2A-Cas9)  
82 (Addgene # 194768), a donor vector for converting Gal4 into Cas9 (KOREMAN *et al.* 2021). The  
83 homology arms (HAs) are 1119 bp for 5' and 1194 bp for 3'. We use two gRNAs targeting the  
84 middle of Gal4 in the donor vector to increase the CRISPR efficiency. To make pHACK(Gal4)-  
85 DONR(T2A-LexAGAD), a nlsLexAGAD partial sequence was PCR amplified from pDEST-  
86 APIC-LexAGAD (POE *et al.* 2017) using oligos  
87 GAAGCGGAGGCgtgcATGCCACCCAAAGAAGAAGC and  
88 CACATATAGGACTTTCTGCAGTCAGTCTATCCAGCTC. The fragment was

89 assembled with NheI/PstI digested pHACK(Gal4)-DONR(T2A-Cas9) through NEBuilder HiFi  
90 DNA Assembly. To make pHACK(Gal4)-DONR(T2A-Flp1), the Flp1 CDS was PCR amplified  
91 from pDEST-APIC-Flp1 (POE *et al.* 2017) and assemble with NheI/AgeI digested  
92 pHACK(Gal4)-DONR(T2A-Cas9) through NEBuilder HiFi DNA Assembly.

93 *13XLexAop2-GFPnls-PEST*

94 A DNA fragment containing SV40 nuclear localization signal (nls) and a protein destabilization  
95 PEST signal from mouse ornithine decarboxylase (NP\_038642.2; corresponding to aa 423-461)  
96 was synthesized (Integrated DNA Technologies, Inc) and cloned into pAPLO (POE *et al.* 2017).  
97 The superfolder GFP (sfGFP) coding sequence was PCR-amplified from pIHEU-AV-sfGFP  
98 (SAPAR *et al.* 2018), with syn21 (a translation enhancer), start codon, and SV40 nuclear  
99 localization signal (nls) in the forward primer, and cloned in-frame before SV40nls and PEST in  
100 pAPLO.

101 *Generation of transgenes*

102 Injections were carried out by Rainbow Transgenic Flies (Camarillo, CA 93012 USA) to  
103 transform flies through φC31 integrase-mediated integration into attP sites. Each HACK donor  
104 vector was inserted into the attP40 (on the 2<sup>nd</sup> chromosome) and attP<sup>VK00027</sup> (on the 3<sup>rd</sup>  
105 chromosome) sites. 13XLexAop2-GFPnlsPEST was inserted into attP<sup>VK00033</sup> site.

106 *Conversion of Gal4 to LexAGAD and Flp*

107 Conversion experiments were conducted similarly to Figure 2. A germline-specific nos-Cas9  
108 (PORT *et al.* 2014) or *Bam-Cas9* (CHEN *et al.* 2020) on the X chromosome was combined with  
109 the appropriate donor transgene and a Gal4 insertion into the same fly through two sequential  
110 crosses. The Gal4 and the donor transgene were located on two homologous chromosomes.  
111 Founder flies containing all three components were crossed to reporter lines. For *nos-Cas9*,  
112 female founders appeared to have higher efficiencies of conversion than male founders. For  
113 *Bam-Cas9*, we used male founders because *Bam-Cas9* was reported to have higher activity in the  
114 male germline (CHEN *et al.* 2020). For Flp conversion, *10XUAS-IVS-mCD8::RFP 13XLexAop2-*  
115 *mCD8::GFP; CoinFLP-LexA::GAD.GAL4* (BDSC # 58754) was initially used as the reporter.  
116 Later, *Tub>STOP>LexAGAD::VP16; 13XLexAop2-6XGFP* was built as a more convenient  
117 reporter. For LexAGAD conversion, *13XLexAop2-6XGFP* (SHEARIN *et al.* 2014) was used as the  
118 reporter. 3<sup>rd</sup> instar larvae showing the expected GFP expression patterns were screened from the  
119 progeny under a Nikon SMZ18 fluorescence stereomicroscope and recovered for development  
120 into adulthood. The resulting flies were crossed to proper balancer stocks to separate the reporter  
121 chromosome and the converted LexAGAD or Flp chromosome. In our hands, it takes  
122 approximately 60 days from the beginning to the establishment of a converted line. A subset of  
123 the converted LexAGAD and Flp lines were validated by genomic PCR (Figure S1).

124 *Validation of expression pattern/imaging*

125 The converted LexAGAD and Flp lines were crossed to GFP reporter lines according to Table 1.  
126 GFP expression patterns in wandering 3<sup>rd</sup> instar larvae were examined with a Leica SP8 confocal  
127 equipped with a 20X oil objective. For brain expressions, we dissected larval brains and stained  
128 the samples with the primary antibody NC82 (Developmental Studies Hybridoma Bank, 1:100)  
129 and the secondary antibody Cy5 donkey anti-mouse antibody (Jackson ImmunoResearch  
130 Laboratories; 1:400) to visualize neuropiles. For wing disc expression, we dissected larvae and  
131 stained the samples with 4',6-diamidino-2-phenylindole (DAPI; 1:36000). For all other crosses,  
132 we imaged the body walls of live larvae.

## 133 Results

### 134 *Construct designs and the principle of conversion*

135 To enable conversion of Gal4 lines into LexA and Flp lines, we generated two HACK donor  
136 transgenic constructs (Figure 1A), building on a dual-gRNA vector we previously optimized for  
137 CRISPR-mutagenesis in the *Drosophila* germline (KOREMAN *et al.* 2021). Each donor construct  
138 carries three functional units that collectively enable homology-directed repair (HDR)-mediated  
139 conversion and larval screening. First, a gRNA cassette encodes two gRNAs driven by two  
140 separate polymerase III promoters (CR7T and U6:3) to target the Gal4 coding sequence. The  
141 gRNAs adopt the gRNA2.1 scaffold (GREVET *et al.* 2018), which is more efficient than the  
142 original and the gRNA(F+E) scaffolds in mutagenesis in mammalian cells and *Drosophila*  
143 (GREVET *et al.* 2018; KOREMAN *et al.* 2021). We used two, instead of only one, gRNAs to  
144 increase the possibility of DNA double-strand break. Second, a donor sequence contains the  
145 coding sequence of 2A-Flp or 2A-LexA flanked by two homology arms (HAs) from the Gal4  
146 coding sequence. While the DNA binding domain of LexA is fused in-frame with the Gal4  
147 activation domain (GAD, within the 3' HA) in the LexA donor construct, the Flp sequence is  
148 followed by a *hsp70* polyA for transcription termination in the Flp donor construct. Third, a  
149 nuclear BFP (nBFP) marker driven by a polyubiquitin promotor (ubi) serves as a selection  
150 marker for distinguishing the donor chromosome. The donor vectors were constructed in pAC  
151 (attB-CaSpeR), a backbone that is compatible with both P-element- and PhiC31-mediated  
152 transformation (HAN *et al.* 2011).

153 The conversion of Gal4 is induced in the *Drosophila* germline by combining the LexA or  
154 Flp donor transgene, a Gal4 of interest, and a germline specific Cas9 (such as *nos-Cas9* and  
155 *bam-Cas9-P2A-Flp*) (Figure 1B). gRNA/Cas9 produces DSBs in the middle of the Gal4 coding  
156 sequence. Homology-directed repair of the DSBs using the donor sequence as a template will  
157 result in in-frame incorporation of 2A-LexA or 2A-Flp in the original Gal4 locus. During  
158 translation, the “self-cleaving” 2A peptide releases a truncated and nonfunctional Gal4 and  
159 LexAGAD or Flp as two separate proteins. Thus, the expression pattern of the resulting  
160 LexAGAD/Flp line should reflect that of the original Gal4.

161 The conversion can be carried out through several simple steps of genetic crosses  
162 (illustrated in Figure 2 for converting Gal4 insertions on the 2<sup>nd</sup> chromosome to LexA versions).

163 Successful conversion events will result in chromosomes that carry tissue-specific LexA or Flp  
164 and can be identified using specific LexA or Flp reporters. We used *13XLexAop2-6XGFP*  
165 (SHEARIN *et al.* 2014) as a LexA reporter and *10XUAS-IVS-mCD8::RFP 13XLexAop2-mCD8::GFP*;  
166 *CoinFLP-LexA::GAD.GAL4* and *Tub>STOP>LexAGAD::VP16*; *13XLexAop2-6XGFP* as Flp  
167 reporters. These reporters express high levels of fluorescent proteins in the Flp/LexA expressing  
168 tissues, making it easy to identify larvae carrying the converted chromosome, even when the  
169 expression domain is restricted. Although our method was designed for converting Gal4 lines  
170 that exhibit recognizable expression patterns in the whole larva, similar approaches should allow  
171 conversion of Gal4 lines that show visible expression patterns in adults.

172 *Conversion of example Gal4 lines*

173 We inserted each donor construct into two attB sites, one on the second chromosome and the  
174 other on the third, through PhiC31-mediated integration. To test the effectiveness of the  
175 conversion, we chose 10 Gal4 lines that show tissue-specific expression in the larva (Table 2).  
176 These Gal4 transgenes are at various locations on the second and the third chromosomes and  
177 were created by diverse means, including enhancer trap (BRAND AND PERRIMON 1993), enhancer  
178 fusion with random insertion (RANGANAYAKULU *et al.* 1998), enhancer fusion with targeted  
179 insertion (PFEIFFER *et al.* 2008), and recombineering of genomic DNA clones followed by  
180 targeted insertion (CHAN *et al.* 2011). These Gal4s are controlled by regulatory sequences from  
181 different genes and are expressed in diverse larval cell types, including epithelial cells, muscles,  
182 neurons, glia, adipocytes, hemocytes, and stem cells.

183 We used donor transgenes located on the same chromosomes as the Gal4 insertions for  
184 conversion. For 14 out of 15 conversion experiments, we were able to identify larvae expressing  
185 the reporter in the expected pattern and to derive fly lines containing the converted chromosome  
186 from these larvae. Although the conversion frequency varied from experiment to experiment  
187 (Table 2), we recovered enough GFP-positive larvae by screening 100-300 candidates. The only  
188 exception was *RabX4-Gal4* to *RabX4-Flp* conversion, in which *bam-Cas9-P2A-Flp* (CHEN *et al.*  
189 2020) produced leaky somatic Flp activity that interfered with the screening. In addition, we also  
190 tested Gal4-to-LexA conversion for *Or22a-Gal4* (Table 2), which has no larval expression but is  
191 expressed in a small number of olfactory neurons in the antenna. Because the adult cuticle is not  
192 transparent, *Or22a-Gal4* represents a challenging test case. We failed to detect obvious GFP  
193 signals in candidate adult flies using our setup.

194 *Comparison of the activity patterns of converted LexAGAD and Flp lines with those of the*  
195 *original Gal4 lines*

196 To evaluate the activity patterns of the resultant LexAGAD and Flp lines, we crossed them to  
197 reporters (Table 1) and compared their activity patterns to those of their corresponding Gal4 lines.  
198 Cytosolic GFP reporters were used for lines that are expressed in non-neural tissues (Figure 3),  
199 while membrane-targeted GFP (mGFP) was used to examine the processes of neurons and glia  
200 (Figures 4A-4B’). Nuclear GFP (nGFP) was used to locate the cell bodies of neurons (for  
201 OK371 and OK319) in the densely packed ventral nerve cord (VNC) (Figures 4C-4D’).

202 The activity patterns of the converted LexAGAD lines faithfully recapitulated the  
203 expression patterns of the corresponding Gal4 lines (Figures 3 and 4), with the only exception of  
204 *wg-LexAGAD*. Although *wg-LexAGAD* has a similar activity pattern as *wg-Gal4* in the larval  
205 epidermis (Figures 3D and 3D'), it showed broader activity in the wing pouch and restricted  
206 expression elsewhere in the wing imaginal disc of the late 3<sup>rd</sup> instar larva as compared to *wg-*  
207 *Gal4* (Figures S2A and S2B). In comparison, two of the five converted Flp lines did not show  
208 identical activity patterns as their Gal4 counterparts. Specifically, *esg-Flp1* did not label all  
209 histoblasts but occasionally showed activity in some tracheal and muscle cells (Figure 3A").  
210 Unlike *wg-Gal4* that is active in a narrow strip of epidermal cells along the dorsal-ventral axis of  
211 each hemisegment (Figure 3D), *wg-Flp1* labeled a smaller cluster of epidermal cells, as well as  
212 few peripheral neurons (arrowhead), in every hemisegment (Figure 3D"). In the wing imaginal  
213 disc, while *wg-Gal4* activity was detected at the dorsal/ventral boundary of the wing disc (Figure  
214 S1A), where *wg* expression is expected (DIAZ-BENJUMEA AND COHEN 1995; KIM *et al.* 1995),  
215 *wg-Flp1* resulted in labeling of distinct cell patches in dorsal and ventral compartments (Figure  
216 S2B). The discrepancies between Gal4 and Flp could be due to different thresholds required for  
217 activating their corresponding reporters and the fact that Flp patterns result from accumulation of  
218 activities throughout the developmental history while Gal4 patterns reflect current activity.

219 **Discussion**

220 HACK is a convenient method for converting one genetic reagent to another through genetic  
221 crosses. With prebuilt donor transgenes, Gal4 can be converted into other reagents without  
222 needing cloning or injection, greatly simplifying the process required for generating new  
223 reagents. Converted reagents in theory should have similar activity patterns as the original Gal4  
224 lines and thus, in most cases, need very little characterization. This method has been successfully  
225 used to convert Gal4 into QF, split Gal4, Gal80, and Cas9. In this study, we further expand the  
226 existing toolbox and make reagents available for generating tissue-specific LexAGAD and Flp  
227 lines from Gal4 lines. This conversion process is straightforward and can be performed in any  
228 *Drosophila* lab that is equipped with a fluorescence dissecting microscope. The ability to expand  
229 the current choices of LexA and Flp reagents to match those available for Gal4 will provide fly  
230 researchers greater flexibility for studying their questions.

231 Our HACK method differs from other similar approaches in the design of the donor  
232 constructs. The first important difference is that we used the CR7T-U63(2.1) design for  
233 expressing dual gRNAs. This design is specifically optimized for the *Drosophila* germline  
234 (KOREMAN *et al.* 2021). With higher mutagenic efficiency in the germline, this design is  
235 predicted to improve the conversion rate. Second, instead of using the 3xP3-RFP marker for  
236 selecting potential convertants (LIN AND POTTER 2016), we rely on LexA- or Flp-dependent  
237 reporter expression as the primary means for identifying the converted chromosomes. Although  
238 3xP3-RFP is more convenient to screen in adults because of RFP expression in the eye, it has  
239 some disadvantages. Because 3xP3-RFP will be carried over into the converted reagents, it may  
240 interfere with subsequent experiments and, in most cases, needs to be first removed by the Cre

241 recombinase. Also, incomplete homologous recombination events can result in false positive  
242 candidates that have incorporated 3xP3-RFP marker but not functional converted reagents (CHEN  
243 *et al.* 2020). In comparison, screening based on reporter expression directly identifies correctly  
244 converted chromosomes and thus does not need additional validation by genomic PCR. The  
245 converted reagents can be directly used in subsequent experiments. The additional ubi-nlsBFP  
246 marker serves as a selection maker for distinguishing the donor chromosome but is not  
247 absolutely needed.

248 Screening KI events based on expression patterns also has some caveats. When Gal4  
249 expressing cells are too sparse or buried too deeply inside the body, especially in adults that have  
250 opaque cuticles, the fluorescence from the expressing cells may not be distinguishable for  
251 screening. For example, we failed to convert *Or22a-Gal4*, which is only expressed in a small  
252 number of olfactory neurons whose cell bodies are buried inside the antenna. In situations like  
253 this, donor templates that incorporate visible selection markers may still be better choices for the  
254 conversion.

255 As reported previously (LIN AND POTTER 2016), the frequency of conversion can vary  
256 greatly among different Gal4 lines, likely due to the local chromatin conformation. We noticed a  
257 wide range of conversion efficiencies as well (Table 2). While *OK371-Gal4* and *dcg-Gal4* were  
258 very easy to convert, *RabX4-Gal4* and *FlyLight* Gal4 lines were more refractory to conversion.  
259 For Gal4 lines that are difficult to convert, the efficiency can be improved by taking several  
260 measures. First, when *nos-Cas9* (PORT *et al.* 2014) is used as the germline Cas9, we found that  
261 female founders, which contain Cas9, Gal4, and the donor transgene, gave higher conversion  
262 rates than male founders. Second, *bam-Cas9-P2A-Flp*, which is expressed in germline precursor  
263 cells but not in germline stem cells, was reported to perform better in germline HDR (CHEN *et al.*  
264 2020). Our preliminary comparisons support this conclusion. Thirdly, even though we have not  
265 confirmed it, using two copies of donor transgenes may improve efficiency as well. The Lee  
266 group recently reported the E-Golic+ for genetic cross-based KI (CHEN *et al.* 2020). This system  
267 incorporates *bam-Cas9-P2A-Flp* and uses induced lethality to eliminate non-converted  
268 chromosomes and thus could dramatically improve the efficiency. Although this system also  
269 requires removing selection markers from positive candidates, it may still be a better choice for  
270 converting Gal4 insertions extremely difficult to convert by other means.

271 Besides HACK, new LexA and Flp reagents can also be generated by other means. For  
272 example, MiMIC (VENKEN *et al.* 2011) and CRIMIC (LEE *et al.* 2018) lines, for which large  
273 collections are available, can be converted into different effectors using appropriate  
274 Recombinase Mediated Cassette Exchange (RMCE) donor lines. The InSITE system (GOHL *et al.*  
275 2011) also allows for effector conversion of >1,300 enhancer-trap Gal4 lines based on RMCE.  
276 Although donor lines for converting these resources into LexA (except for InSITE) and Flp  
277 reagents still need to be established, these systems offer complementary approaches for  
278 expanding LexA and Flp choices. Lastly, although the enhancer-fusion Gal4 lines in the FlyLight  
279 (JENETT *et al.* 2012) and VT (KVON *et al.* 2014) collections are compatible with HACK, we

280 found that these Gal4 transgenes inserted into the attP2 site are relatively more difficult to  
281 convert by HACK. Because the enhancer sequence for each of these Gal4 lines is molecularly  
282 defined, making and transforming new enhancer-fusion constructs may be a more reliable  
283 approach for generating corresponding LexA and Flp strains (POE *et al.* 2017).

284 The HACK method can in principle be used to convert Gal4 into any other type of  
285 genetic reagent. Although we present tools for generating LexA and Flp in this study, our donor  
286 vectors can be modified for conversion of many other types of reagents, such as GeneSwitch-  
287 Gal4 (OSTERWALDER *et al.* 2001), LexA::P65 (PFEIFFER *et al.* 2010), cpf1 (ZETSCHÉ *et al.* 2015),  
288 etc.

289

290 **Table 1. Crosses for validating Gal4, LexAGAD, and Flp activity patterns.**

Gal4 name	Gal4 reporter	LexA reporter	Flp1 reporter
OK371	UAS-GFPnls	13XLexAop2-GFPnls	-
OK319	UAS-GFPnls	13XLexAop2-GFPnls	-
esg-Gal4	UAS-GFP	13XLexAop2-6XGFP	Tub>STOP>LexAGAD::VP16; 13XLexAop2-6XGFP
Mef2-Gal4	UAS-GFP	13XLexAop2-6XGFP	-
dcg-Gal4	UAS-GFP	13XLexAop2-6XGFP	-
wg-Gal4	UAS-GFP	13XLexAop2-6XGFP	Tub>STOP>LexAGAD::VP16; 13XLexAop2-6XGFP
RabX4-Gal4	UAS-CD4-tdGFP	13XLexAop2-CD4-GFP	-
repo-Gal4	UAS-CD4-tdGFP	13XLexAop2-CD4-GFP	Tub>STOP>LexAGAD::VP16; 13XLexAop2-6XGFP
R16D01-Gal4	UAS-GFP	-	Tub>STOP>LexAGAD::VP16; 13XLexAop2-6XGFP
R28E04-Gal4	UAS-GFP	13XLexAop2-6XGFP	Tub>STOP>LexAGAD::VP16; 13XLexAop2-6XGFP

291 **Table 2. Summary of Gal4 lines and conversion rates**

Gal4	Chr. Arm	Gene	Gal4 expression pattern in larva	LexA rate	Flp rate
OK371	2L	<i>VGlut</i>	glutamatergic neurons	25/80 (f) 9/118 (m)	N.A.
OK319	2		motor neuron subset	N.C.	N.A.
esg-Gal4	2L	<i>esg</i>	imaginal tissues; histoblasts	5/76 (f)	5-15/150 (m)
Mef2-Gal4	3	<i>Mef2</i>	somatic muscles	N.C.	N.A.

dcg-Gal4	2		the fat body; hemocytes	73/147 (f) 4/78 (m)	N.A.
wg-Gal4	2L	<i>wg</i>	epidermal cell subset; imaginal tissue subset	N.C.	5-15/150 (m)
RabX4-Gal4	3L	<i>RabX4</i>	all neurons	6/146 (f)	Failed*
repo-Gal4	3R	<i>repo</i>	glia	N.C.	5-15/150 (m)
R16D01-Gal4	3L	<i>wg</i>	epidermal cell subset; imaginal tissue subset	N.A.	5-15/150 (m)
R28E04-Gal4	3L	<i>hh</i>	epidermal cell subset; imaginal tissue subset	N.C.	5-15/150 (m)
Or22a-Gal4	2	<i>Or22a</i>	adult Or22a olfactory sensory neurons**	Failed	N.A.

292 LexA conversion was performed using *nos-Cas9*; Flp conversion was performed using *bamP-Cas9-P2A-Flp*. The conversion rates, when available, are presented as # GFP-positive larvae/#  
293 total BFP-negative larvae. (f): conversion using female founders (flies containing Cas9, donor  
294 transgene, and Gal4); (m): conversion using male founders. N.C.: Not counted. N.A.: Not  
295 attempted. \*The Gal4-to-Flp conversion for *RabX4-Gal4* failed because bam-CF has leaky Flp  
296 activity outside of the germline that interfered with screening of *RabX4-Flp*. We did not attempt  
297 the conversion again using a different Cas9. \*\*Or22a-Gal4 has no larval expression.  
298

299

## 300 Data Availability

301 The donor vectors are available at Addgene: pHACK(Gal4)-DONR(T2A-LexAGAD) (Addgene  
302 # 194769); pHACK(Gal4)-DONR(T2A-Flp1) (Addgene # 194770). Other plasmids are available  
303 upon request. *Drosophila* strains are available at Bloomington *Drosophila* Stock Center or upon  
304 request. The authors affirm that all data necessary for confirming the conclusions of the article  
305 are present within the article, figures, and tables.

## 306 Acknowledgments

307 We thank Tzumin Lee, Bloomington *Drosophila* Stock Center (NIH P40OD018537), and  
308 KYOTO Stock Center for fly stocks; Dion Dickman and members of Han lab for critical reading  
309 and suggestions on the manuscript. This work was supported by NIH grants (R01NS099125,  
310 R21OD023824, and R24OD031953) awarded to C.H..

## 311 Author Contributions

312 S.K., A.T.Y., B.W., and C.H. designed research; S.K., A.T.Y., B.W., and P.F.G. performed  
313 research; B.W. contributed new reagents/analytic tools; S.K., A.T.Y., and C.H. analyzed data;  
314 C.H. wrote the manuscript; S.K., A.T.Y., and C.H. edited the manuscript; C.H. acquired funding.

315 **Declaration Of Interests**

316 The authors declare no competing financial interests.

317 **Reference**

318 Bischof, J., R. K. Maeda, M. Hediger, F. Karch and K. Basler, 2007 An optimized transgenesis  
319 system for Drosophila using germ-line-specific phiC31 integrases. *Proc Natl Acad Sci U  
320 S A* 104: 3312-3317.

321 Bosch, J. A., G. Birchak and N. Perrimon, 2021 Precise genome engineering in Drosophila using  
322 prime editing. *Proc Natl Acad Sci U S A* 118.

323 Bosch, J. A., R. Colbeth, J. Zirin and N. Perrimon, 2020 Gene Knock-Ins in Drosophila Using  
324 Homology-Independent Insertion of Universal Donor Plasmids. *Genetics* 214: 75-89.

325 Brand, A. H., and N. Perrimon, 1993 Targeted gene expression as a means of altering cell fates  
326 and generating dominant phenotypes. *Development* 118: 401-415.

327 Chan, C. C., S. Scoggin, D. Wang, S. Cherry, T. Dembo *et al.*, 2011 Systematic discovery of Rab  
328 GTPases with synaptic functions in Drosophila. *Curr Biol* 21: 1704-1715.

329 Chen, H. M., X. Yao, Q. Ren, C. C. Chang, L. Y. Liu *et al.*, 2020 Enhanced Golic+: highly  
330 effective CRISPR gene targeting and transgene HACKing in Drosophila. *Development*  
331 147.

332 Dang, D. T., and N. Perrimon, 1992 Use of a yeast site-specific recombinase to generate  
333 embryonic mosaics in Drosophila. *Dev Genet* 13: 367-375.

334 Diaz-Benjumea, F. J., and S. M. Cohen, 1995 Serrate signals through Notch to establish a  
335 Wingless-dependent organizer at the dorsal/ventral compartment boundary of the  
336 Drosophila wing. *Development* 121: 4215-4225.

337 Ewen-Campen, B., D. Yang-Zhou, V. R. Fernandes, D. P. Gonzalez, L. P. Liu *et al.*, 2017  
338 Optimized strategy for in vivo Cas9-activation in Drosophila. *Proc Natl Acad Sci U S A*  
339 114: 9409-9414.

340 Gohl, D. M., M. A. Silies, X. J. Gao, S. Bhalerao, F. J. Luongo *et al.*, 2011 A versatile in vivo  
341 system for directed dissection of gene expression patterns. *Nat Methods* 8: 231-237.

342 Golic, K. G., and S. Lindquist, 1989 The FLP recombinase of yeast catalyzes site-specific  
343 recombination in the Drosophila genome. *Cell* 59: 499-509.

344 Gratz, S. J., A. M. Cummings, J. N. Nguyen, D. C. Hamm, L. K. Donohue *et al.*, 2013 Genome  
345 engineering of Drosophila with the CRISPR RNA-guided Cas9 nuclease. *Genetics* 194:  
346 1029-1035.

347 Gratz, S. J., F. P. Ukkenn, C. D. Rubinstein, G. Thiede, L. K. Donohue *et al.*, 2014 Highly  
348 specific and efficient CRISPR/Cas9-catalyzed homology-directed repair in Drosophila.  
349 *Genetics* 196: 961-971.

350 Grevet, J. D., X. Lan, N. Hamagami, C. R. Edwards, L. Sankaranarayanan *et al.*, 2018 Domain-  
351 focused CRISPR screen identifies HRI as a fetal hemoglobin regulator in human  
352 erythroid cells. *Science* 361: 285-290.

353 Han, C., L. Y. Jan and Y. N. Jan, 2011 Enhancer-driven membrane markers for analysis of  
354 nonautonomous mechanisms reveal neuron-glia interactions in Drosophila. *Proc Natl  
355 Acad Sci U S A* 108: 9673-9678.

356 Huang, P., P. Sahai-Hernandez, R. A. Bohm, W. P. Welch, B. Zhang *et al.*, 2014 Enhancer-trap  
357 flippase lines for clonal analysis in the Drosophila ovary. *G3 (Bethesda)* 4: 1693-1699.

358 Jenett, A., G. M. Rubin, T. T. Ngo, D. Shepherd, C. Murphy *et al.*, 2012 A GAL4-driver line  
359 resource for Drosophila neurobiology. *Cell Rep* 2: 991-1001.

360 Kim, J., K. D. Irvine and S. B. Carroll, 1995 Cell recognition, signal induction, and symmetrical  
361 gene activation at the dorsal-ventral boundary of the developing *Drosophila* wing. *Cell* 82:  
362 795-802.

363 Koreman, G. T., Y. Xu, Q. Hu, Z. Zhang, S. E. Allen *et al.*, 2021 Upgraded CRISPR/Cas9 tools  
364 for tissue-specific mutagenesis in *Drosophila*. *Proc Natl Acad Sci U S A* 118.

365 Kvon, E. Z., T. Kazmar, G. Stampfel, J. O. Yanez-Cuna, M. Pagani *et al.*, 2014 Genome-scale  
366 functional characterization of *Drosophila* developmental enhancers *in vivo*. *Nature* 512:  
367 91-95.

368 Lai, S. L., and T. Lee, 2006 Genetic mosaic with dual binary transcriptional systems in  
369 *Drosophila*. *Nat Neurosci* 9: 703-709.

370 Lee, P. T., J. Zirin, O. Kanca, W. W. Lin, K. L. Schulze *et al.*, 2018 A gene-specific T2A-GAL4  
371 library for *Drosophila*. *Elife* 7.

372 Lee, T., and L. Luo, 1999 Mosaic analysis with a repressible cell marker for studies of gene  
373 function in neuronal morphogenesis. *Neuron* 22: 451-461.

374 Lin, C. C., and C. J. Potter, 2016 Editing Transgenic DNA Components by Inducible Gene  
375 Replacement in *Drosophila melanogaster*. *Genetics* 203: 1613-1628.

376 Luan, H., N. C. Peabody, C. R. Vinson and B. H. White, 2006 Refined spatial manipulation of  
377 neuronal function by combinatorial restriction of transgene expression. *Neuron* 52: 425-  
378 436.

379 McGuire, S. E., P. T. Le, A. J. Osborn, K. Matsumoto and R. L. Davis, 2003 Spatiotemporal  
380 rescue of memory dysfunction in *Drosophila*. *Science* 302: 1765-1768.

381 Nern, A., B. D. Pfeiffer, K. Svoboda and G. M. Rubin, 2011 Multiple new site-specific  
382 recombinases for use in manipulating animal genomes. *Proc Natl Acad Sci U S A* 108:  
383 14198-14203.

384 Neukomm, L. J., T. C. Burdett, M. A. Gonzalez, S. Zuchner and M. R. Freeman, 2014 Rapid *in*  
385 *vivo* forward genetic approach for identifying axon death genes in *Drosophila*. *Proc Natl  
386 Acad Sci U S A* 111: 9965-9970.

387 Osterwalder, T., K. S. Yoon, B. H. White and H. Keshishian, 2001 A conditional tissue-specific  
388 transgene expression system using inducible GAL4. *Proc Natl Acad Sci U S A* 98:  
389 12596-12601.

390 Pfeiffer, B. D., A. Jenett, A. S. Hammonds, T. T. Ngo, S. Misra *et al.*, 2008 Tools for  
391 neuroanatomy and neurogenetics in *Drosophila*. *Proc Natl Acad Sci U S A* 105: 9715-  
392 9720.

393 Pfeiffer, B. D., T. T. Ngo, K. L. Hibbard, C. Murphy, A. Jenett *et al.*, 2010 Refinement of tools  
394 for targeted gene expression in *Drosophila*. *Genetics* 186: 735-755.

395 Poe, A. R., L. Tang, B. Wang, Y. Li, M. L. Sapar *et al.*, 2017 Dendritic space-filling requires a  
396 neuronal type-specific extracellular permissive signal in *Drosophila*. *Proc Natl Acad Sci  
397 U S A* 114: E8062-E8071.

398 Port, F., H. M. Chen, T. Lee and S. L. Bullock, 2014 Optimized CRISPR/Cas tools for efficient  
399 germline and somatic genome engineering in *Drosophila*. *Proc Natl Acad Sci U S A* 111:  
400 E2967-2976.

401 Potter, C. J., B. Tasic, E. V. Russler, L. Liang and L. Luo, 2010 The Q system: a repressible  
402 binary system for transgene expression, lineage tracing, and mosaic analysis. *Cell* 141:  
403 536-548.

404 Ranganayakulu, G., D. A. Elliott, R. P. Harvey and E. N. Olson, 1998 Divergent roles for NK-2  
405 class homeobox genes in cardiogenesis in flies and mice. *Development* 125: 3037-3048.

406 Sapar, M. L., H. Ji, B. Wang, A. R. Poe, K. Dubey *et al.*, 2018 Phosphatidylserine  
407 Externalization Results from and Causes Neurite Degeneration in Drosophila. *Cell Rep*  
408 24: 2273-2286.

409 Sharma, Y., U. Cheung, E. W. Larsen and D. F. Eberl, 2002 PPTGAL, a convenient Gal4 P-  
410 element vector for testing expression of enhancer fragments in drosophila. *Genesis* 34:  
411 115-118.

412 Shearin, H. K., I. S. Macdonald, L. P. Spector and R. S. Stowers, 2014 Hexameric GFP and  
413 mCherry reporters for the Drosophila GAL4, Q, and LexA transcription systems.  
414 *Genetics* 196: 951-960.

415 Struhl, G., and K. Basler, 1993 Organizing activity of wingless protein in Drosophila. *Cell* 72:  
416 527-540.

417 Venken, K. J., K. L. Schulze, N. A. Haelterman, H. Pan, Y. He *et al.*, 2011 MiMIC: a highly  
418 versatile transposon insertion resource for engineering Drosophila melanogaster genes.  
419 *Nat Methods* 8: 737-743.

420 Xie, T., M. C. W. Ho, Q. Liu, W. Horiuchi, C. C. Lin *et al.*, 2018 A Genetic Toolkit for  
421 Dissecting Dopamine Circuit Function in Drosophila. *Cell Rep* 23: 652-665.

422 Xu, T., and G. M. Rubin, 1993 Analysis of genetic mosaics in developing and adult Drosophila  
423 tissues. *Development* 117: 1223-1237.

424 Zetsche, B., J. S. Gootenberg, O. O. Abudayyeh, I. M. Slaymaker, K. S. Makarova *et al.*, 2015  
425 Cpf1 is a single RNA-guided endonuclease of a class 2 CRISPR-Cas system. *Cell* 163:  
426 759-771.

427

428 **Figure Legend**

429 **Figure 1. Construct designs and the principle of conversion**

430 (A) Diagrams of Flp and LexA HACK donor constructs. The vectors were constructed in pAC, a  
431 dual-transformation backbone (via PhiC31 and P-transposase) that carries a mini-white selection  
432 marker. See text for descriptions of other components. pA: polyA tail; TS: gRNA target  
433 sequence; P: P-element.

434 (B) Diagram of Gal4-to-Flp/LexA conversion using a HACK donor line. The donor expresses  
435 two gRNAs (TS1 and TS2) targeting the tissue-specific (ts) Gal4, which results in in-frame  
436 incorporation of 2A-Flp/LexA into the Gal4 locus through homology-directed repair (HDR). The  
437 donor expresses *ubi-nBFP* that can be selected against when screening for convertants.

438 **Figure 2. Example crossing scheme for converting Gal4 into LexAGAD**

439 Illustrated is a crossing scheme for converting a second-chromosome Gal4 line into LexAGAD  
440 line. The most critical step is the screening of convertants based on fluorescence in the expected  
441 pattern (Step 3). 50-300 larvae, depending on the Gal4, usually need to be screened to get  
442 enough convertant candidates (5-10 larvae). This particular example utilizes *nos-Cas9* as the  
443 germline Cas9 and a donor transgene on the second chromosome. *nos-Cas9* is more effective in  
444 female founders than in males. *nos-Cas9* can be substituted by *bam-Cas9-P2A-Flp*, which is  
445 more effective in male founders than in females. The donor transgene can also be on a  
446 nonhomologous chromosome.

447 **Figure 3. Comparison of Gal4 and converted LexA and Flp lines in non-neural tissues**

448 (A-A'') Activity patterns of *esg-Gal4* (A), *esg-LexAGAD* (A'), and *esg-Flp1* (A'') in the whole  
449 larval body.

450 (B-B') Activity patterns of *Mef2-Gal4* (B) and *Mef2-LexAGAD* (B') in the whole larval body.

451 (C-C') Activity patterns of *Dcg-Gal4* (C) and *Dcg-LexAGAD* (C') in the whole larval body.

452 (D-D'') Activity patterns of *wg-Gal4* (D), *wg-LexAGAD* (D'), and *wg-Flp1* (D'') in epidermal  
453 cells of a single hemisegment. Arrowhead (D'') indicates the cell body of a sensory neuron.

454 (E-E'') Activity patterns of *R28E04-Gal4* (E), *R28E04-LexAGAD* (E'), and *R28E04-Flp1* (E'') in  
455 epidermal cells of a single hemisegment.

456 (F-F'') Activity patterns of *R16D01-Gal4* (F) and *R16D01-LexAGAD* (F') in epidermal cells of a  
457 single hemisegment.

458 Refer to Table 1 for reporter lines used. Scale bar: 300  $\mu$ m (A-C'); 100  $\mu$ m (D-F').

459 **Figure 4. Comparison of Gal4 and converted LexA and Flp lines in the nervous system**

460 (A-A') Activity patterns of *RabX4-Gal4* (A) and *RabX4-LexAGAD* (A') in a single dorsal  
461 hemisegment.

462 (B-B') Activity patterns of *repo-Gal4* (B), *repo-LexAGAD* (B'), and *repo-Flp1* (B'') in a single  
463 dorsal hemisegment.

464 (C and C') Activity patterns of *OK371-Gal4* (C) and *OK371-LexAGAD* (C') in the larval brain.

465 (D and D') Activity patterns of *OK319-Gal4* (D) and *OK319-LexAGAD* (D') in the larval brain.

466 Refer to Table 1 for reporter lines used. Scale bar: 100  $\mu$ m in all panels.

467 **Figure S1. Validation of converted LexAGAD and Flp lines by genomic PCR**

468 (A) Diagram of converted Flp transgene and genomic PCR results for *esg*, *repo*, and *wg* lines.  
469 The positions of 5' and 3' homology arms (HAs), binding locations of PCR primers, and  
470 expected sizes of PCR products are indicated in the diagram. The DNA gel shows PCR results of  
471 the Flp donor line, the original Gal4 (1), and the converted Flp (2).

472 (B) Diagram of converted LexAGAD transgene and genomic PCR results for *repo*, *OK371*, and  
473 *wg* lines. The diagram and PCR results are labeled similarly to (A).

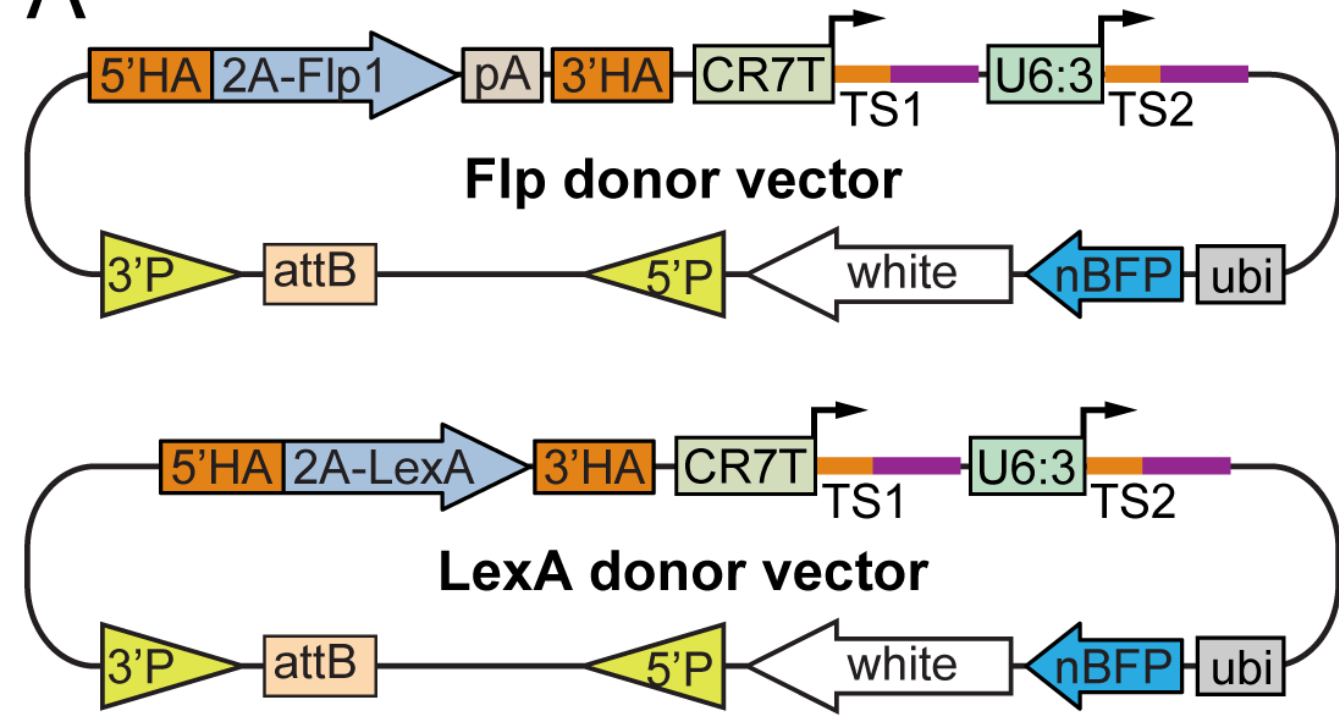
474 The primers used for PCR amplifications are (a) CTTGAAGCAAGCCTCCTGAAAG; (b)  
475 AGTGGTATTAAACATCCCTGTAGTG; (c) TGACGCACCAACACCTTG; (d)  
476 CAGGAGGTTCTGGATTACCTGAG; (e) GAGAGCCTCATTGGATCTTCTAC; (f)  
477 ACCATCTACCACGGTATCATTGAG.

478 **Figure S2. Comparison of *wg-Gal4*, *wg-LexAGAD*, and *wg-Flp* lines in the wing disc**

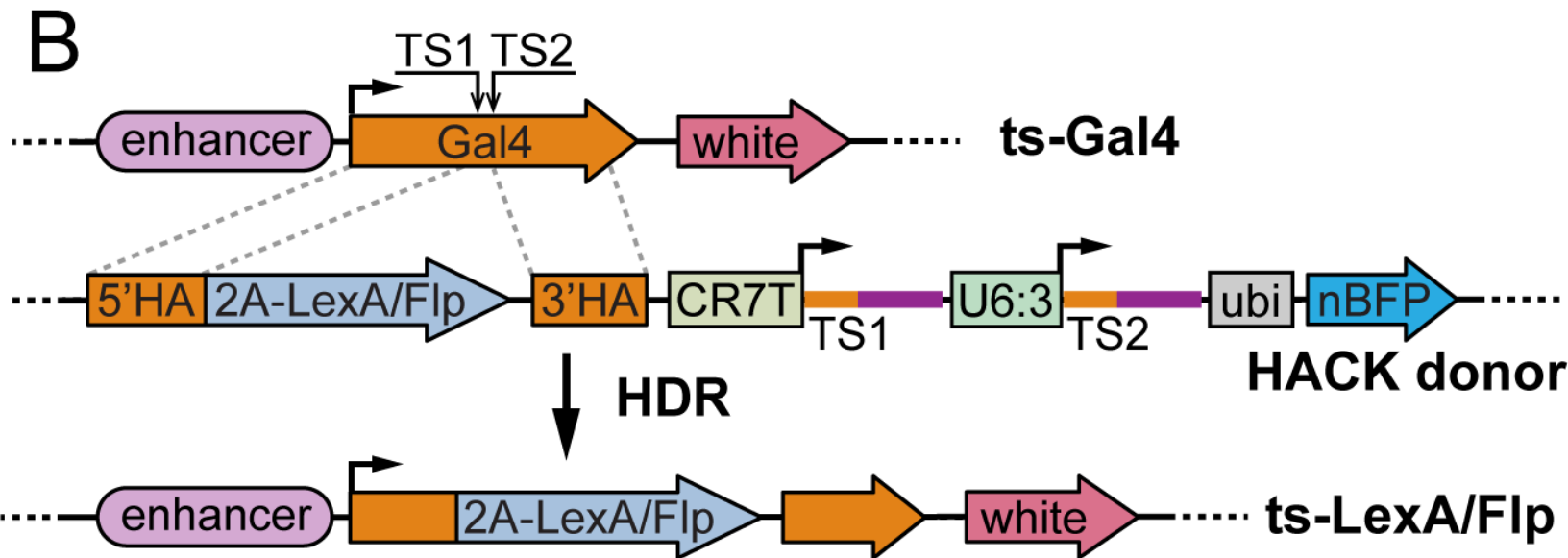
479 (A-C) Activity patterns of *wg-Gal4* (A), *wg-LexAGAD* (B), and *wg-Flp1* (C) in a 3<sup>rd</sup> instar wing  
480 imaginal disc. GFP is in green; DAPI staining is in blue.

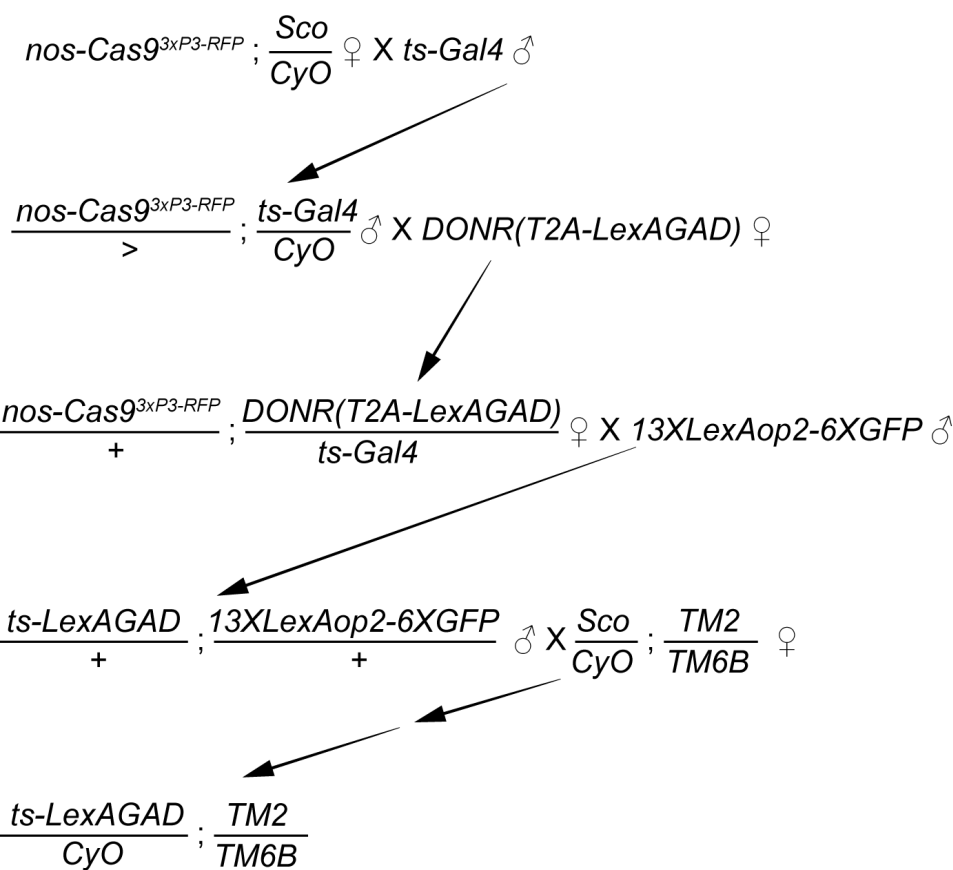
481 Refer to Table 1 for reporter lines used. Scale bar: 100  $\mu$ m in all panels.

A



B





**Step 1. Combine nos-Cas9 and Gal4 into one fly**

**Step 2. Combine nos-Cas9, Gal4, and donor into one fly**

- DONR(T2A-LexAGAD) expresses ubiquitous nuclear BFP
- screen for CyO- RFP+ females

**Step 3. Screen for convertants**

- screen for larvae that express GFP in the expected pattern;
- select against RFP and BFP;
- keep male adults for next cross

**Step 4. Isolate converted chromosome**

- cross male convertants individually to balancer line
- separate ts-LexAGAD and 13XLexAop2-6XGFP (e.g. by chromosome association)
- establish stable lines

